(29) Fowler, R. H.; Rushbrooke, G. S. *Trans. Faraday Soc.* **1933**, *33*, 1272.
(30) Chang, T. S. *Proc. Cambridge R. Soc.* **1939**, *35*, 265.
(31) Miller, A. R. *Proc. Cambridge R. Soc.* **1942**, *38*, 109.
(32) Orr, W. J. C. *Trans. Faraday Soc.* **1944**, *40*, 307.
(33) Flory, P. J. *J. Chem. Phys.* **1941**, *9*, 660.
(34) Flory, P. J. *Proc. R. Soc. London, A* **1956**, *234*, 60.
(35) Flory, P. J. *Proc. Natl. Acad. Sci. U.S.A.* **1942**, *79*, 4510.
(36) Kurata, M.; Tamura, M.; Watari, T. *J. Chem. Phys.* **1955**, *23*, 991.
(37) Freed, K. F.; Bawendi, M. G. *J. Phys. Chem.* **1989**, *93*, 2194.
(38) Okamoto, H. *J. Chem. Phys.* **1979**, *70*, 1690.
(39) Bellemans, A.; De Vos, E. *J. Polym. Sci., Part C, Polym. Symp.* **1973**, *42*, 1195.
(40) Dickman, R.; Hall, C. K. *J. Chem. Phys.* **1986**, *85*, 3023.
(41) Irvine, P.; Gordon, M. *Macromolecules* **1980**, *13*, 761.
(42) Longuet-Higgins, H. C. *Proc. R. Soc. London* **1951**, *A205*, 247.
(43) Jones, J. E.; Ingham, A. E. *Proc. R. Soc. London* **1925**, *A107*, 636.
(44) Koningsveld, R.; Kleintjens, L. A. *Macromolecules* **1971**, *4*, 637.
(45) Nies, E.; Koningsveld, R.; Kleintjens, L. A. *Prog. Colloid Polym. Sci.* **1985**, *17*, 2.
(46) Nanda, V. S.; Simha, R.; Somcynsky, T. *J. Polym. Sci., Part C, Polym. Symp.* **1966**, *12*, 277.
(47) See ref 1, pp 323-334.
(48) Quach, A.; Simha, R. *J. Appl. Phys.* **1971**, *42*, 4592.
(49) Olabisi, O.; Simha, R. *Macromolecules* **1975**, *8*, 205.
(50) Walsh, D. J. Central Research and Development Department, E. I. du Pont de Nemours & Co. Inc., Wilmington, DE 19898, private communication.
(51) Hillegers, L. T. M. E. The estimation of parameters in functional relationship models. Dissertation, 1986, Eindhoven University of Technology, The Netherlands.
(52) Olabisi, O.; Simha, R. *Macromolecules* **1975**, *8*, 211.

A Modified Hole Theory of Polymeric Fluids. 2. Miscibility Behavior and Pressure Dependence of the System Polystyrene/Cyclohexane

Alexander Stroeks and Erik Nies*

Department of Polymer Technology, Eindhoven University of Technology, 5600MB Eindhoven, The Netherlands

Received November 2, 1989; Revised Manuscript Received March 15, 1990

ABSTRACT: Experimental miscibility behavior and the influence of pressure upon it are discussed with the modified hole theory introduced in the previous paper. For the first time the complicated pressure dependence for the system polystyrene/cyclohexane is theoretically reproduced. The modified hole theory and Simha-Somcynsky hole theory are compared. Thermodynamically the pressure dependence of the critical temperature is related to the compositional curvature of the volume of mixing. According to the modified hole theory a complicated composition dependence for the volume of mixing is predicted as a result of a delicate interplay of two volume effects. Spanning the complete composition range a volume contraction is predicted directly related to the change in the structure parameter defined in the hole theory. However, this overall contraction is perturbed by a volume expansion related to the packing efficiency of different component segments. These two distinct volume contributions result in a complicated dependence of the volume of mixing on composition and set the hole theories apart from other equation-of-state theories currently available.

Introduction

Since the pioneering work of Flory,[1-3] Huggins,[4-6] and Prigogine,[7] a vast number of publications has been devoted to the study of upper (UCMT) and lower critical miscibility temperature (LCMT) phase behavior in relation to different thermodynamic and molecular parameters. Basically, for nonpolar polymer systems (thus excluding systems with strong orientation-dependent interactions) the UCMT demixing is a result of entropic contributions to the free energy favoring miscibility at high temperatures and unfavorable energetic interactions ultimately causing the system to demix at sufficiently low temperatures.[8] The entropically driven LCMT demixing is essentially due to a mismatch between the equation-of-state properties of the constituents.[8] The discussion of strong orientational interactions can be successful only when different theoretical concepts are applied.[7,9] Therefore, in the present paper only nonpolar systems will be discussed. The basic ingredients, i.e., combinatorial entropy and energetic and equation-of-state contributions, not only provide a sound theoretical framework to discuss phase behavior at atmospheric pressure but also allow the evaluation of, e.g., excess functions and the influence of pressure on thermodynamic properties. Independent of any particular model, thermodynamic correlations of course exist between the excess enthalpy and volume and the pressure dependence on the phase behavior.[8] These correlations bring to bear a thorough test upon the molecular theories at hand. Partly to test these relations the influence of pressure on the phase behavior for different polymer solutions and blends has been documented experimentally.[10-12] Some current theories are not capable of correlating these data.[10,11] In this work the Simha-Somcynsky hole theory[13] and a modified hole theory[14] are used to discuss the experimental data. With the modified hole theory a consistent prediction of all the data available for the system polystyrene/cyclohexane is obtained.

Theory

A. Helmholtz Free Energy. The hole theory for pure components discussed in the previous paper[14] is readily extended to mixtures. For a binary mixture of N_a and N_b molecules of component A and B, respectively, in a volume

0024-9297/90/2223-4092$02.50/0

V, the configurational Helmholtz free energy reads

$$\begin{aligned} A/(NsRT) = {} & \phi_a \ln(\phi_a)/s_a + \phi_b \ln(\phi_b)/s_b + \\ & (1-y)\ln(1-y)/y + \ln(y)/\langle s\rangle - \\ & (1-\langle\alpha\rangle y)\ln(1-\langle\alpha\rangle y)/(\gamma y) - \langle c_s\rangle \ln(\langle v^*\rangle Q(1-\eta)^3) + \\ & (1-\langle\alpha\rangle) y\langle c_s\rangle (AQ^{-4} - 2BQ^{-2})/(2(1-\langle\alpha\rangle y)\tilde{T}) \end{aligned} \quad (1)$$

where ϕ_a ($=1-\phi_b$) $= N_a s_a/(N_a s_a + N_b s_b)$; s_a and s_b are the relative chain lengths of components A and B; y is the occupied site fraction; $\langle s\rangle$ is the average chain length; $\langle\alpha\rangle = \gamma(1 - 1/\langle s\rangle)$; $\gamma = 2/z$; z is the lattice coordination number; $\langle c_s\rangle$ is the average flexibility parameter; $\langle v^*\rangle$ is the average segmental hard-core volume; $Q = y\tilde{V}$; $\eta = 2^{-1/6}y(1-\langle\alpha\rangle)/((1-\langle\alpha\rangle y)Q^{1/3})$; $\tilde{V}$ and $\tilde{T}$ are the reduced volume and temperature, respectively; and A (=1.011) and B (=1.2045) are geometrical constants. For $\langle\alpha\rangle = 0$ eq 1 reduces to the expression given by Jain and Simha.[15] Equation 1 is very similar to eq 17 in ref 14. The differences are (1) an extra combinatorial entropy contribution due to mixing different components and (2) composition-averaged molecular parameters. Following Prigogine, Bellemans, and Englert-Chwoles,[16] the composition averages for the potential parameters $\langle\epsilon^*\rangle$ and $\langle v^*\rangle$ are obtained from the principle of corresponding states and can be computed from

$$\langle\epsilon^*\rangle\langle v^*\rangle^m = \epsilon^*_{aa}v^{*\,m}_{aa}q_a^{\,2} + 2\epsilon^*_{ab}v^{*\,m}_{ab}q_a q_b + \epsilon^*_{bb}v^{*\,m}_{bb}q_b^{\,2}; \quad m = 2, 4 \quad (2)$$

where ϵ^*_{aa}, ϵ^*_{bb}, v^*_{aa}, and v^*_{bb} are related to the interactions between segments of identical molecules and ϵ^*_{ab} and v^*_{ab} are cross parameters defining the interaction between segments of A and B molecules.

The external contact fraction q_a ($=1 - q_b$) is defined according to $q_a = \phi_a(1 - \gamma(1 - 1/s_a))/(1 - \gamma(1 - 1/\langle s\rangle))$.

From the partition function for the binary system the composition dependences of the average chain length $\langle s\rangle$ and the number of external degrees of freedom $\langle c_s\rangle$ are obtained from

$$1/\langle s\rangle = \phi_a/s_a + \phi_b/s_b \quad (3)$$

$$\langle c_s\rangle = \phi_a c_{sa} + \phi_b c_{sb} \quad (4)$$

where c_{sa} and c_{sb} refer to components A and B, respectively.

B. Equation of State. From the Helmholtz free energy all configurational thermodynamic properties can be obtained. The equation of state is defined by the pressure equation $p = -(\partial A/\partial V)_{N,T,y}$ and the minimization condition $(\partial A/\partial y)_{N,T,V}$. In terms of reduced variables these equations read

$$\tilde{P}\tilde{V}/\tilde{T} = 1/(1-\eta) + 2(1-\langle\alpha\rangle)y(AQ^{-4} - BQ^{-2})/(1-\langle\alpha\rangle y)\tilde{T} \quad (5)$$

$$\begin{aligned} 0 = {} & (3\eta - 1 + \langle\alpha\rangle y)/((1-\eta)(1-\langle\alpha\rangle y)) + \\ & (1-\langle\alpha\rangle)y[2BQ^{-2} - 3AQ^{-4} + 4\langle\alpha\rangle y(AQ^{-4} - BQ^{-2})]/ \\ & 2\tilde{T}(1-\langle\alpha\rangle y)^2 - \langle c_s\rangle(\ln(1-y)/y + 1 - \\ & 1/\langle s\rangle - \ln(1-\langle\alpha\rangle y)/(\gamma y) - \langle\alpha\rangle/\gamma) \end{aligned} \quad (6)$$

The reducing parameters P^*, V^*, and T^* are functions of the composition-dependent molecular parameters according to

$$P^* = z(1-\langle\alpha\rangle)\langle\epsilon^*\rangle/\langle v^*\rangle \quad (7a)$$

$$V^* = \langle s\rangle\langle v^*\rangle \quad (7b)$$

$$T^* = z(1-\langle\alpha\rangle)\langle\epsilon^*\rangle/\langle c_s\rangle R \quad (7c)$$

C. Phase Behavior: Spinodal and Critical Conditions. Generally, in the P-V-T-ϕ_b space of a binary system a two-phase region or miscibility gap exists bounded by the binodal condition. The miscibility gap is subdivided by the spinodal in a metastable and unstable region. Binodal and spinodal make contact at the critical state, which for strictly binary systems is situated at the top of both curves. In the following we will consider upper critical miscibility temperature (UCMT) and lower critical miscibility temperature (LCMT) phase behavior. For the present discussion we limit ourselves to the computation of spinodal and consolute conditions for binary mixtures. The spinodal condition is defined by[17]

$$J_{sp} = \partial^2 G/\partial\phi_b^{\,2}|_{P,T} = 0 \quad (8)$$

where $G = A + pV$ is the Gibbs free energy.

At the consolute state the spinodal condition (8) is obeyed simultaneously with the extra condition

$$J_{cr} = \partial^3 G/\partial\phi_b^{\,3}|_{P,T} = 0 \quad (9)$$

D. Influence of Pressure. The change with pressure of the critical temperature, $(\partial T/\partial P)_c$, and the change with pressure of the critical composition, $(\partial\phi_b/\partial P)_c$, are given by[8]

$$(\partial T/\partial P)_c = T_c(\partial^2 V/\partial\phi_b^{\,2})_c/(\partial^2 H/\partial\phi_b^{\,2})_c \quad (10)$$

$$(\partial\phi_b/\partial P)_c = \frac{(\partial^3 S/\partial\phi_b^{\,3})_c(\partial^2 V/\partial\phi_b^{\,2})_c - (\partial^3 V/\partial\phi_b^{\,3})_c(\partial^2 S/\partial\phi_b^{\,2})_c}{(\partial^2 S/\partial\phi_b^{\,2})_c(\partial^4 G/\partial\phi_b^{\,4})_c} \quad (11)$$

Furthermore, the curvature of the enthalpy of mixing as a function of composition is related to the type of phase behavior:[8]

$$\text{UCMT:}\quad (\partial^2 H/\partial\phi_b^{\,2})_c < 0 \quad (12a)$$

$$\text{LCMT:}\quad (\partial^2 H/\partial\phi_b^{\,2})_c > 0 \quad (12b)$$

By combining eqs 10 and 12 the slope of the critical temperature with pressure is directly related to the curvature of the volume of mixing as a function of composition. If the excess volume and enthalpy of mixing have uniform curvature spanning the complete composition space, the sign of the curvature is opposite to the sign of the excess function. Consequently, the sign of the coefficient $(\partial T/\partial p)_c$ can be related to the sign of the critical excess volume ΔV_c and enthalpy ΔH_c of mixing:

$$\text{sign}((\partial T/\partial P)_c) = T_c\,\text{sign}(\Delta V_c)/\text{sign}(\Delta H_c) \quad (13)$$

In most cases little is known about the compositional curvature of excess functions, and eq 13 is adopted as a first approximation.

Comparison with Experimental Data and Discussion

A. Selected Experimental Data. For the system polystyrene/cyclohexane (PS/CH) a wealth of accurate experimental data from different laboratories is available. A selection from these data will be used to illustrate the positions of the SS and HH hole theories. The available molecular characteristics and supplier information for solvents and polymers are shown in Table I. All polymers are anionically polymerized with a narrow molar mass distribution (MMD). For three PS fractions UCMT

Table I
Available Molecular Characteristics and Supplier Information for Selected Samples and Solvents

sample	$10^{-3}M_w$	M_w/M_n	supplier
PS M1	51	1.04	Pressure Chemical
PS M2	166	1.08	Pressure Chemical
PS M3	520	1.19	Pressure Chemical
PS M4	600	<1.10	Pressure Chemical
PS M5	37	<1.06	Pressure Chemical
PS M6	110	<1.06	Pressure Chemical
PS M7	670	<1.15	Pressure Chemical
PS M8	1450	<1.10	Pressure Chemical
PS M9	97	<1.06	Pressure Chemical
PS M10	200	<1.06	Pressure Chemical
PS M11	400	<1.06	Pressure Chemical
PS M12	670	<1.10	Pressure Chemical
PS M13	2700	<1.10	Pressure Chemical
CH1			
CH2			spectrochemical quality
CH3			Merck

Table II
Spinodal Data for PS Fractions M1, M2, and M3 in Cyclohexane[18]

T_{spin}, K	$w_{PS,spin}$	T_{spin}, K	$w_{PS,spin}$
	PS M1/CH1		
279.55	0.0258	288.45	0.2029
284.75	0.0435	287.35	0.0756
287.35	0.0764	288.25	0.0894
288.25	0.0903	288.95	0.1194
288.95	0.1204	289.05	0.1404
289.05	0.1415	288.95	0.1707
288.95	0.1721	288.45	0.2013
	PS M2/CH1		
289.95	0.0186	295.55	0.1496
294.25	0.0407	296.05	0.0617
296.05	0.0620	296.35	0.0817
296.35	0.0821	296.45	0.1008
296.45	0.1012	296.25	0.1230
296.25	0.1243	295.55	0.1489
	PS M3/CH1		
297.55	0.0175	300.45	0.0635
299.65	0.0289	300.15	0.0832
300.45	0.0450	299.55	0.1046
300.55	0.0540		

Table III
Critical Coordinates for PS Fractions M1, M2, and M3 in Cyclohexane[19]

sample	T_{crit}, K	$w_{PS,crit}$
PS M1/CH1	288.85	0.146
PS M2/CH1	296.60	0.099
PS M3/CH1	301.15	0.064

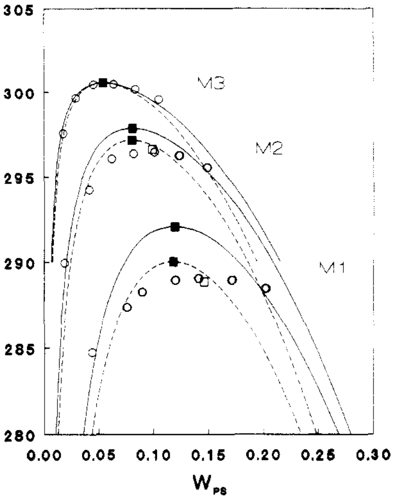

Figure 1. Experimental spinodal[18] (○) and critical[19] data (□) for the systems M1, M2, and M3 in CH1. Predicted critical coordinates (■) and spinodal curves according to SS (- - -) and HH (—) theories.

Table IV
Experimental LCMT Cloud Point Data for PS Fractions M12, M7, M11, M10, M9, and M5 in Cyclohexane[a]

T, K	w_{PS}	T, K	w_{PS}
	PS M12/CH2		
489.13	0.0180	488.81	0.0351
488.60	0.0224	491.08	0.0605
	PS M7/CH2		
491.78	0.0070	491.77	0.0362
492.10	0.0143	491.93	0.0655
491.74	0.0275	492.39	0.0733
	PS M11/CH2		
497.27	0.0023	495.01	0.0279
495.36	0.0218	494.49	0.0810
	PS M10/CH2		
497.32	0.0306	496.82	0.1039
496.93	0.0565	497.38	0.1327
496.89	0.0972	498.12	0.1524
	PS M9/CH2		
503.81	0.0247	501.83	0.1041
502.52	0.0503	501.97	0.1229
502.02	0.0753	502.21	0.1520
	PS M5/CH2		
511.44	0.0537	510.42	0.1589
510.86	0.0806	512.44	0.2276
510.70	0.1060	513.11	0.2325

[a] Data are obtained from the original figure in ref 20.

spinodal[18] and critical[19] data are given in Tables II and III and shown in Figure 1. Experimental LCMT cloud point data for a different set of PS molar masses[20] are shown in Table IV and Figure 2. In Table V the critical temperature as a function of pressure is tabulated in the pressure range 0–300 bar. These data were obtained by Wolf and Geerissen[10] for a molar mass of 600 kg/mol. Finally, for a set of molar masses ranging from 37 to 2700 kg/mol Saeki, Kuwahara, Nakata, and Kaneko[11] determined the critical temperature as a function of pressure. The pressure interval covered in these experiments ranges from 0 to 50 bar. These data are summarized in Table VI.

B. Determination of Molecular Parameters. To confront SS and HH hole theories with experimental data, estimates for the molecular parameters are needed. The pure-component parameters are determined from experimental equation-of-state data.[21,22] The mixture cross parameters ϵ^*_{ab} and v^*_{ab} are obtained from the consolute condition for the system M3/CH1. The complete sets of molecular parameters for HH and SS theories are summarized in Table VII. Using these values for the molecular parameters, we are now in a position to predict any desired thermodynamic property for the system PS/CH. The requisite expressions for the evaluation of binodals and spinodals, following from eq 1, have been previously derived.[23]

C. Predicted Thermodynamic Properties. 1. Spinodal and Critical Conditions: Atmospheric Pressure. The predicted critical coordinates for the polymer samples M1 and M2 and spinodal conditions for the PS fractions M1, M2, and M3 are compared to experimental results in Figure 1. For the HH theory the calculated change of critical temperature and composition with molar mass is too small. For SS theory the agreement with experimental data is better. It has been shown previously that small

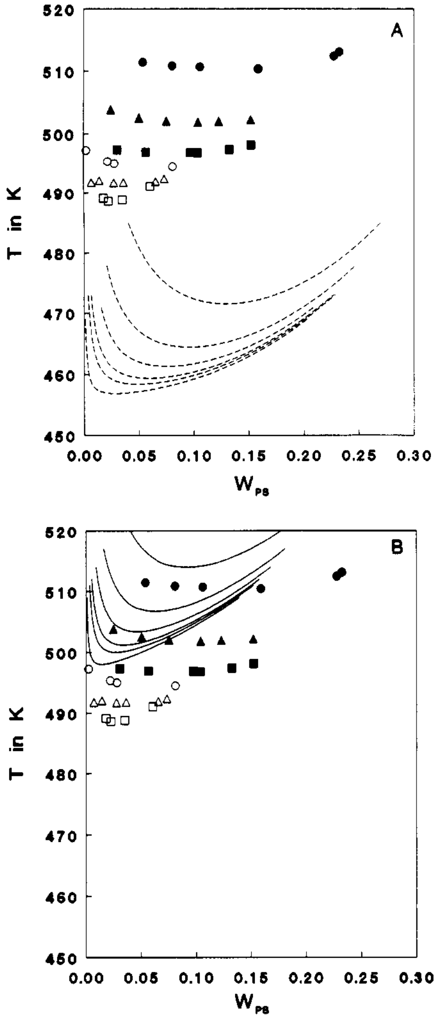

Figure 2. Experimental LCMT cloud point data[20] for different molar masses (M5 (●), M9 (▲), M10 (■), M11 (○), M7 (△), and M12 (□)) and predicted spinodal curves according to (A) SS (- - -) and (B) HH (—) theories.

Table V
Experimental Critical Temperatures versus Pressure for the PS Fractions M4 in Cyclohexane[a]

T_{crit}, K	P, bar	T_{crit}, K	P, bar
	PS M4/CH3		
301.34	1	301.12	187
301.11	37	301.43	260
300.95	88	301.68	300
300.96	152		

[a] Data are extracted from the original figure in ref 10.

changes with molar mass in the molecular parameters ϵ^*_{ab} and v^*_{ab} can correct the deviations between theoretical and experimental critical coordinates.[24] Also, predicted and experimental spinodal curves are in reasonable agreement, and the observed systematic deviations can be rationalized. Differences between experimental and theoretical spinodal branches at the left-hand side of the critical point are related to dilute-solution effects. The present hole theories are derived for uniform segment densities. In dilute solutions large fluctuations in the local segment concentration exist, thus violating the uniform segment density approximation.[25-26] These dilute-solution effects have been discussed in the literature based on different theoretical concepts.[18,27-39] In principle, the hole theories can be corrected for such dilute-solution effects, but this will not be discussed here. The right-hand side of the calculated spinodal branches is somewhat too narrow in comparison with experimental data. These differences can be reconciled by allowing small changes in the flexibility parameter,[24] which can be interpreted as a slight temperature dependence.

Table VI
Experimental Critical Temperatures versus Pressure for PS Fractions M5, M6, M7, and M8 in Cyclohexane[a]

P, bar	UCST, K	P, bar	UCST, K
	PS M5/CH2		
1	285.41	30	285.49
10	285.43	40	285.53
20	285.46	50	285.56
	PS M6/CH2		
1	294.38	30	294.36
10	295.36	40	294.35
20	294.35	50	294.35
	PS M7/CH2		
1	300.97	30	300.81
10	300.91	40	300.79
20	300.86	50	300.75
	PS M8/CH2		
1	303.27	30	303.10
10	303.21	40	303.04
20	303.15	50	302.98

[a] Data are extracted from the original figures in ref 11.

Table VII
Molecular Parameters for PS and CH According to the SS and HH Theories[a]

	ϵ^*, J/mol	v^*, m^3/mol	c_s	$10^{-3}M_0$
PS				
SS	6968.8	9.9538×10^{-5}	0.76939	0.104
HH	6690.9	9.8464×10^{-5}	0.85312	0.104
CH	6543.4	9.3596×10^{-5}	1.8	0.08416
	Cross Parameters			
SS	6727.8203	$9.71528991 \times 10^{-5}$		
HH	6559.4962	$9.66737305 \times 10^{-5}$		

[a] Pure-component parameters are estimated from experimental PVT data.[21,22] The cross interaction parameters are estimated from the critical condition for the system M3/CH.[19]

For the present discussion was are primarily interested in the pressure dependence of the phase behavior. Therefore we do not make the parameters molar mass or temperature dependent to improve the correspondence between theory and experiment but will proceed with the single set of molecular parameters summarized in Table VII extracted from pure-component PVT data and a single UCMT critical point. In Figure 2 the predicted and experimental LCMT phase behavior for the data of Saeki et al. are compared. The agreement between theory and experiment is satisfactory, particularly if one realizes that with the set of molecular parameters estimated from a energetically driven phenomenon situated at a temperature of ca. 300 K, an entropy-driven demixing 180 K higher is predicted with this accuracy. Also here the change of the critical coordinates with molar mass is slightly underestimated. This is comparable to the situation observed for the UCMT behavior. The shape of calculated LCMT spinodal and experimental LCMT cloud point curves cannot be compared directly. However, similar conclusions as for the UCMT behavior may be expected. Comparison of the spinodal curves calculated according to HH and SS theories reveals differences between the models. For the HH theory the LCMT miscibility gaps are predicted at higher temperatures, in better agreement with experimental data. Furthermore, the spinodal curves according to SS theory are considerably broader than the corresponding HH curves.

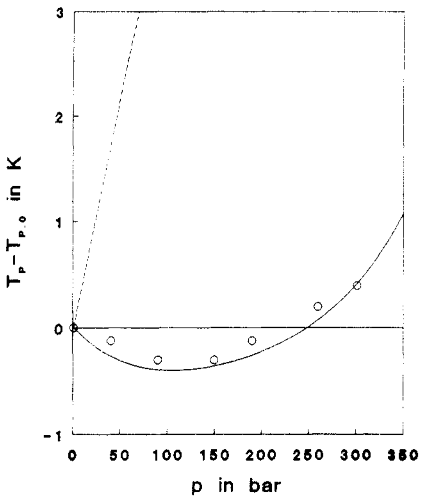

Figure 3. Differences between critical temperatures at elevated and atmospheric pressure versus pressure. Experimental data[10] (○) and predicted pressure dependence according to SS (- - -) and HH (—) theories.

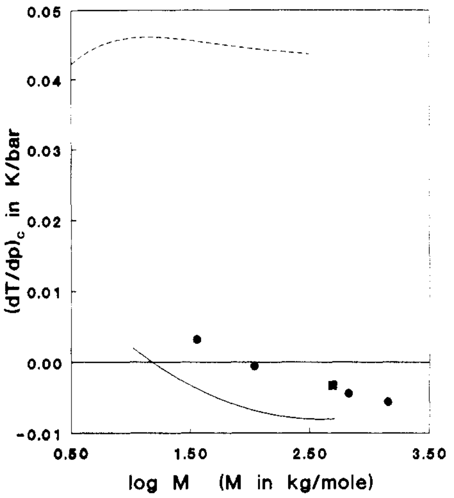

Figure 4. Pressure coefficient $(\partial T/\partial P)_c$ versus the logarithm of molar mass. Experimental data of Saeki et al.[11] (●) and Wolf and Geerissen[10] (■). Predicted pressure coefficient $(\partial T/\partial P)_c$ according to SS (- - -) and HH (—) theories.

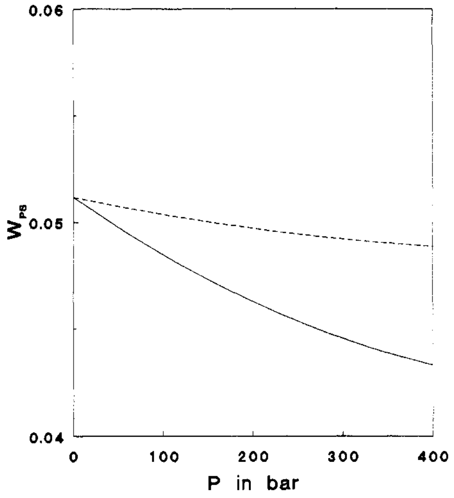

Figure 5. Predicted pressure dependence of the critical composition according to SS (- - -) and HH (—) theories.

It is well recognized that LCMT demixing is governed by free-volume differences between the constituents.[40] In the hole theories discussed here this quantity is explicitly defined in terms of the structure parameter $h = (1 - y)$, i.e., the free-site fraction. The improved miscibility predictions according to the HH theory are realized because of a smaller difference in this quantity.[15,23] That is, phase separation is therefore predicted at higher temperatures in the HH than in the SS theory.

2. Influence of Pressure. In Figure 3 calculated and experimental critical coordinates can be compared for the data of Wolf and Geerissen. As indicated by the previous results, one may expect deviations between calculated and experimental data at atmospheric pressure merely due to theory. Furthermore, as shown by Wolf and Geerissen, even in solvents of different suppliers, different critical temperatures are obtained.[10] Therefore the pressure dependence of the critical temperature is shown in Figure 3 relative to the critical temperature at atmospheric pressure. SS theory predicts a monotonous increase of the critical temperature with pressure, and the predicted slope is ca. 10 times too large. The modified hole theory, however, gives an excellent prediction of the observed effect. Slope and change in sign are predicted by the HH theory. With this theory a consistent prediction of the experimental data of Saeki et al. is realized also.

In Figure 4 the initial slope of the critical temperature is drawn as a function of the logarithm of the molar mass. In this figure the experimental results of Wolf and Geerissen and Saeki et al. are combined. The computed and measured values of the slope differ by approximately a constant amount for all molar masses. On the other hand, the molar mass dependence is predicted quite well. Consequently, the exact value of the molar mass at which the slope changes sign is not predicted accurately. However, one has to realize that all these predictions are obtained with mixture parameters determined from a single critical temperature and composition at atmospheric pressure. The results shown in Figure 3 and 4 demonstrate quite clearly that the modified hole theory gives a very good prediction of these subtle pressure phenomena.

For completeness, the change of critical composition with pressure for UCMT and LCMT phase behavior is shown in Figure 5. According to eq 11 these changes are related to the fourth compositional derivative of the free energy. This is one of the rare experiments that probes the compositional dependency of the free energy in such an intricate manner. However, presently no systematic experimental study for polymer solutions is available. It must be anticipated that, if the small changes predicted are in agreement with experiment, they will be extremely difficult to measure. Once more these calculations reveal differences between the two hole theories. Experimental verification or contradiction would give an extra indication of their relevance.

3. Correlation with Excess Volume and Enthalpy of Mixing. The influence of pressure on the critical temperature is determined by the volume and enthalpy of mixing. In most cases the approximate eq 13 is used to rationalize the experimental data shown in Figures 3 and 4. Accordingly, for the UCMT phase behavior the excess volume of mixing should change sign with pressure and molar mass to explain the subtle changes observed in Figures 3 and 4. However, no exact experimental evidence is available to support these conclusions. For the PS fraction M4 the calculated excess volume of mixing is shown in Figure 6 as a function of pressure at the corresponding critical temperatures.

The excess volume of mixing does not change sign, in disagreement with eq 13. Therefore the exact eq 11 should be used. The change in slope observed in Figure 3 is related to a local change in curvature in the excess volume.

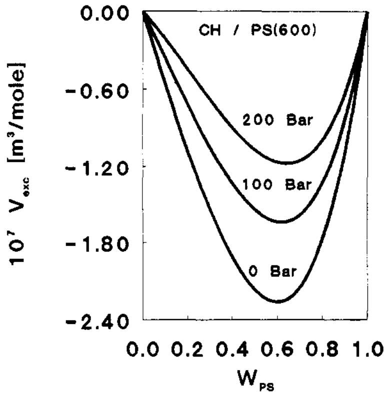

Figure 6. Predicted excess volume of mixing at indicated pressures and corresponding critical temperatures according to HH (—) theory.

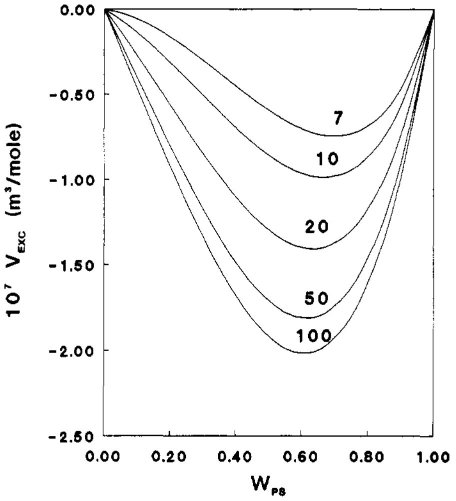

Figure 7. Predicted excess volume of mixing at atmospheric pressure for indicated molar masses (kg/mol) at corresponding critical temperatures according to HH hole theory (—).

Upon applying pressure a change in curvature develops at the low-composition side of the diagram. Therefore, at a certain composition an inflection point exists connecting regions of different curvature. If pressure is increased, the inflection point moves toward higher polymer concentrations. At the point where the pressure coefficient in Figure 3 becomes equal to zero the inflection point coincides with the critical composition. Upon increasing the pressure even more, the inflection point shifts further to higher polymer concentrations, and the critical composition is then situated in the region with negative curvature. Also the data in Figure 4 are explained according to the HH theory by local changes in curvature now initiated by a change in molar mass. This is drawn in Figure 7. At sufficiently high molar mass the situation sketched previously is valid. If the molar mass is decreased, the curvature changes locally. Depending on the location of the inflection point and critical composition, the coefficient $(\partial T/\partial P)_c$ will be positive or negative. For the molar mass at which the inflection point coincides with the critical composition the coefficient $(\partial T/\partial P)_c$ becomes equal to zero.

At present these predictions cannot be compared to experimental data. A more detailed evaluation of the pressure and molar mass dependence of excess functions in relation to the pressure dependence of the critical temperature will be presented in a future paper. Here it suffices to say that the predictions and correlations in this paper seem to be confirmed by experiment. The local changes in the excess volume of mixing are accomplished by an interplay between changes in the structure parameter y, the occupied site fraction, and changes in the cell volume which are related to the packing efficiency of different segments. The unique combination of these two effects is essential to the hole theories discussed in this work and sets them apart from other equation-of-state theories currently available. In modern theories for low molar mass molecular liquids it is well accepted that the liquid structure and properties are determined by geometrical constraints.[41] This effect is accounted for in a first approximation in the SS and HH theories.

Conclusions

Both HH and SS theories are able to describe and predict the phase behavior of polymer solutions. The merits of the theories have been demonstrated for the system PS/CH. Differences between the theories remain relatively small if one is concerned with the UCST and LCST miscibility behavior at atmospheric pressure. However, important differences appear is one is interested in the influence of pressure. For the LCST phase behavior no detailed experimental information is available. Both theories predict an increased miscibility with pressure that can be related to a reduced difference in free volume between components upon applying pressure. For the UCST phase behavior, significant differences between theories emerge. Particularly, the HH theory is very successful in predicting subtle pressure phenomena observed for the UCMT. Thermodynamically the pressure dependence of the critical temperature can be related to the composition dependence of the volume of mixing. In the original literature presenting the experimental data, these subtle changes were correlated with changes in sign of the excess volume of mixing. For the system PS/CH detailed experimental evidence supporting these conclusions is lacking. In this paper we present an alternative and original correlation between the influence of pressure on the critical temperature and the excess volume of mixing. According to the HH theory the excess volume of mixing at the UCMT remains negative but has a rather complicated composition-dependent curvature. Because the experimental data are missing, these predictions cannot now be checked. However, in a forthcoming paper the prediction will be tested with new experimental data. So far, the predictions seem to be confirmed by these new experiments. The theoretical explanation offered by the hole theories is unique and sets them apart from other equation-of-state theories presently available.

Acknowledgment. A.S. gratefully acknowledges support by the Netherlands Foundation for Chemical Research (SON) with financial aid from the Netherlands Organization for Scientific Research (NWO).

References and Notes

(1) Flory, P. J. *J. Chem. Phys.* **1941**, *9*, 660.
(2) Flory, P. J. *Proc. R. Soc. London, A* **1956**, *234*, 60.
(3) Flory, P. J. *Proc. Natl. Acad. Sci. U.S.A.* **1942**, *79*, 4510.
(4) Higgins, M. L. *J. Chem. Phys.* **1941**, *9*, 440.
(5) Huggins, M. L. *J. Phys. Chem.* **1942**, *46*, 151.
(6) Huggins, M. L. *Ann. N.Y. Acad. Sci.* **1943**, *44*, 431.
(7) Prigogine, I.; Bellemans, A.; Mathot, V. *The Molecular Theory of Solutions*; North-Holland Publishing Co.: Amsterdam, 1957; pp 305–322.
(8) Prigogine, I.; Defay, R. *Chemical Thermodynamics*; Longmans and Green: London, 1954; pp 284–290.
(9) Sanchez, I. C.; Balasz, A. C. *Macromolecules* **1989**, *22*, 2325.
(10) Wolf, B. A.; Geerissen, H. *Colloid Polym. Sci.* **1981**, *259*, 1214.
(11) Saeki, S.; Kuwahara, N.; Nakata, M.; Kaneko, M. *Polymer* **1975**, *16*, 445.

4098 *Macromolecules* **1990**, *23*, 4098–4107

(12) Suzuki, Y.; Miyamoto, Y.; Miyaji, H.; Asai, K. *J. Polym. Sci., Polym. Lett. Ed.* **1982**, *20*, 563.
(13) Simha, R.; Somcynsky, T. *Macromolecules* **1969**, *2*, 341.
(14) Nies, E.; Stroeks, A. *Macromolecules*, preceding paper in this issue.
(15) Jain, R. K.; Simha, R. *Macromolecules* **1984**, *17*, 2663.
(16) Prigogine, I.; Bellemans, A.; Englert-Chwoles, A. *J. Chem. Phys.* **1956**, *24*, 518.
(17) Gibbs, J. W. *Collected Works*; Yale University Press: New Haven, 1948; Vol. 1.
(18) Irvine, P.; Gordon, M. *Macromolecules* **1980**, *13*, 761.
(19) Koningsveld, R.; Kleintjens, L. A.; Shultz, A. R. *J. Polym. Sci., Part A2*, **1970**, *8*, 1261.
(20) Saeki, S.; Kuwahara, N.; Konno, S.; Kaneko, M. *Macromolecules* **1973**, *6*, 246.
(21) Quach, A.; Simha, R. *J. Appl. Phys.* **1971**, *42*, 4592.
(22) Jonas, J.; Hasha, D.; Huang, S. G. *J. Phys. Chem.* **1980**, *84*, 109.
(23) Nies, E.; Stroeks, A.; Simha, R.; Jain, R. K., accepted for publication in *J. Colloid Polym. Sci.*
(24) Stroeks, A.; Nies, E. *Polym. Eng. Sci.* **1988**, *28*, 1347.
(25) Flory, P. J. *J. Chem. Phys.* **1945**, *13*, 453.
(26) Flory, P. J. *Principles of Polymer Chemistry*; Cornell University Press: Ithaca, NY, 1953; Chapter VII, XII.
(27) Zimm, B. H. *J. Chem. Phys.* **1946**, *14*, 164.
(28) Flory, P. J.; Krigbaum, W. R. *J. Chem. Phys.* **1950**, *18*, 1086.
(29) Casassa, E. F.; Markovitz, H. *J. Chem. Phys.* **1958**, *29*, 493.
(30) Yamakawa, H. *Modern Theory of Polymer* Solutions; Harper and Row: New York, 1971; Chapter IV.
(31) Fixman, M. *J. Chem. Phys.* **1960**, *33*, 370.
(32) Fixman, M.; Peterson, J. M. *J. Am. Chem. Soc.* **1964**, *86*, 3524.
(33) Edwards, S. F. *Proc. Phys. Soc. London* **1966**, *88*, 265.
(34) Koningsveld, R.; Stockmayer, W. H.; Kennedy, J. W.; Kleintjens, L. A. *Macromolecules* **1974**, *7*, 73.
(35) Des Cloizeaux, *J. Phys. (Les Ulis, Fr.)* **1981**, *42*, 635.
(36) Knoll, A.; Schäfer, L.; Witten, T. A. *J. Phys. (Les Ulis, Fr.)* **1981**, *42*, 767.
(37) Schäfer, L. *Macromolecules* **1982**, *15*, 652.
(38) Ohta, T.; Oono, Y. *Phys. Lett. A* **1982**, *89A*, 460.
(39) Muthukumar, M.; Edwards, S. F. *J. Chem. Phys.* **1982**, *76*, 2720.
(40) McMaster, L. P. *Macromolecules* **1973**, *6*, 760.
(41) Chandler, D. *Studies in Statistical Mechanics*; Montroll, E. W., Lebowitz, J. L., Eds.; North-Holland Publishing Co.: Amsterdam, 1982; Vol. VIII, pp 275–340.

A New Multiplet-Cluster Model for the Morphology of Random Ionomers

A. Eisenberg,* B. Hird,† and R. B. Moore

Department of Chemistry, McGill University, Montreal, P.Q., H3A 2K6, Canada

Received December 7, 1989; Revised Manuscript Received February 21, 1990

ABSTRACT: A new morphological model for random ionomers is proposed which incorporates the findings of recent dynamic mechanical and X-ray scattering studies. The model is based on the existence of multiplets, which reduce the mobility of the polymer chains in their vicinity. The thickness of the restricted mobility layer surrounding each multiplet is postulated to be of the order of the persistance length of the polymer. Isolated multiplets act as large cross-links, thus increasing the glass transition temperature of the material. As the ion content is increased, the regions of restricted mobility surrounding each multiplet overlap to form larger contiguous regions of restricted mobility. When these regions become sufficiently large, they exhibit phase-separated behavior and are termed clusters. The model is in good agreement with a very wide range of experimentally observed phenomena, especially those based on dynamic mechanical and X-ray scattering techniques.

1. Introduction

Over the past two decades, a considerable amount of research has been devoted to random ionomers due to their unique physical properties.[1-13] A number of models for the morphology of random ionomers have been proposed, none of which are completely consistent with all of the experimental observations on these materials. These models have been reviewed recently.[10,11] It is now generally accepted that the ion pairs aggregate to form quadruplets, sextuplets, and higher aggregates, collectively called multiplets.[14] In addition, ion-rich regions termed clusters may also exist at sufficiently high ion contents in some systems.[14] The clusters behave as a separate phase in that they exhibit their own glass transition temperature (T_g). However, the exact structures of the multiplets and clusters have not yet been fully elucidated. In this paper, a new multiplet-cluster model is proposed, which is based on restricted mobility of the polymer chains in the vicinity of the multiplets and which reconciles some of the apparent inconsistencies in our current understanding of these systems.

The first qualitative model for the morphologies of random ionomers was developed by Bonotto and Bonner in 1968.[15] In the same year, Longworth and Vaughan[16] proposed a model based on the analysis of small-angle X-ray scattering (SAXS) data for poly(ethylene-*co*-methacrylic acid) and its alkali-metal ionomer derivatives. A peak corresponding to a Bragg spacing of ca. 50 Å was observed in the scattering profiles. This "ionic" peak was interpreted as being due to scattering from ordered hydrocarbon chains *between* ionic aggregates rather than the aggregates themselves. This model was shown to have several shortcomings, among which are its inability to account for the fact that cesium salts show a much more intense SAXS peak than lithium salts, as well as the observation that both the melting point and the degree of crystallinity are approximately the same in the acid copolymers and the corresponding salt forms.

---

* To whom all correspondence should be addressed.

† Presented as part of a dissertation by B. Hird in partial fulfillment of the Ph.D. degree requirements.

0024-9297/90/2223-4098$02.50/0